
You Had One Job: Per-Task Quantization Using LLMs’ Hidden Representations

Amit LeVi¹ Raz Lapid² Rom Himelstein¹ Yaniv Nemcovsky¹ Ravid Shwartz Ziv³ Avi Mendelson¹

Abstract

Large Language Models (LLMs) excel across diverse tasks, yet many applications require only limited capabilities, making large variants inefficient in memory and latency. Existing approaches often combine distillation and quantization, but most post-training quantization (PTQ) methods are task-agnostic, ignoring how task-specific signals are distributed across layers. In this work, we propose to use hidden representations that encode task-salient signals as a guideline for quantization. In order to fully utilize our innovative idea, this paper compares two new task-aware PTQ methods: **Task-Aware Quantization (TAQ)**, which allocates bitwidths using task-conditioned statistics from hidden activations, and **TAQO**, which allocates precision based on direct layer sensitivity tests. From a small calibration set, these approaches identify task-relevant layers, preserving their precision while aggressively quantizing the rest. This yields stable task sensitivity profiles and efficient task-specialized models. Across models, TAQ and TAQO outperform the baselines; TAQ leads on Phi-4, while TAQO leads on Llama-3.1, Qwen3, and Qwen2.5. For instances, on Phi-4 it achieves 42.33 EM / 50.81 F1, far surpassing Activation-aware Weight Quantization (AWQ) (2.25 / 7.07), while remaining within $\leq 1.0\%$ of the original accuracy at lower average precision.

1. Introduction

Large language models (LLMs) built on the Transformer architecture (Vaswani et al., 2017) continue to scale in size and capability, with empirical scaling laws showing system-

atic improvements as parameter counts grow (Kaplan et al., 2020; Hoffmann et al., 2022). Yet this scaling also amplifies inference- and memory-side costs (Dao et al., 2022; Kwon et al., 2023), making serving efficiency a first-order bottleneck for deployed systems.

Many applications, however, require only a narrow subset of LLM capabilities—for example, code completion (Chen et al., 2021; Roziere et al., 2023), mathematical reasoning (Cobbe et al., 2021b; Hendrycks & et al., 2021), or domain-specific question answering (Tsatsaronis et al., 2015). This motivates fine-tuning and distillation to tailor models to specific tasks (Hu et al., 2021; Ouyang et al., 2022; Sanh et al., 2019; Hinton et al., 2015), typically at the cost of additional training cycles and ongoing maintenance. Quantization is a complementary approach: it reduces memory and latency without heavy training, enabling rapid, low-cost deployment (Gholami et al., 2021; Zhu et al., 2023). For LLMs, progress spans post-training weight rounding with high numerical fidelity (Sharify et al., 2024; Frantar et al., 2022), methods for handling activation outliers or redistributing precision (Dettmers et al., 2022; Xiao et al., 2023), and mixed-precision strategies under global bitwidth budgets (Dong et al., 2019; Lin et al., 2023a).

Concurrently, representation-level studies show that linear directions in hidden states or parameters can encode controllable semantics—such as activation addition (Turner et al., 2024), task vectors (Bowen et al., 2024; Zeng et al., 2025), and models’ safety mechanisms (Arditi et al., 2024; Levi et al., 2025a)—and further indicate that task-salient signals concentrate in specific layers or subspaces, whereas other layers carry more generic features (Song et al., 2024; Zhang et al., 2024; Li et al., 2024; Skean et al., 2025). This evidence motivates using the same salience signals to drive per-task, per-layer distillation (Zhou et al., 2024; Ni et al., 2025).

In contrast, prevailing post training quantization (PTQ) pipelines are task-agnostic: they optimize layer-wise criteria—such as weight error, activation range, or curvature—rather than end-task performance (Nagel et al., 2020; Banner et al., 2019; Wang et al., 2020; Lin et al., 2023a). Consequently, bit precision is often assigned using uniform or manually specified schemes that ignore task importance, rather than prioritizing critical layers. This design can under-

¹Technion – Israel Institute of Technology, Haifa, Israel ²DeepKeep.ai, Tel Aviv, Israel ³Center for Data Science, New York University, New York, USA. Correspondence to: Amit LeVi <amitlevi@campus.technion.ac.il>, Raz Lapid <raz.lapid@deepkeep.ai>, Rom Himelstein <romh@campus.technion.ac.il>, Yaniv Nemcovsky <yanemcovsky@gmail.com>, Ravid Shwartz Ziv <ravidziv@gmail.com>, Avi Mendelson <mendelson@technion.ac.il>.

allocate precision where it matters and over-allocate where it does not, and it typically omits objectives that preserve task-salient hidden representations during quantization (Skean et al., 2025).

In this work, we ask whether task-salient signals in hidden activations can guide post-training quantization. Unlike prevailing PTQ pipelines—which are task-agnostic and rely on local error surrogates over generic calibration data—we propose **Task-Aware Quantization (TAQ)** and its oracle variant **TAQO**, frameworks that convert task-calibrated activations into per-layer precision decisions. Concretely, TAQ computes layer relevance scores from hidden representations on a task-specific calibration set, then solves a budgeted, monotone bit-allocation problem that assigns higher precision to the most task-relevant layers while aggressively quantizing the rest. TAQO, by contrast, bypasses surrogates and allocates precision by directly measuring per-layer task sensitivity. Our contributions are:

- **TAQ**: a PTQ framework that derives layer relevance from task-calibrated hidden activations and allocates bitwidths under an explicit budget.
- **TAQO**: a task-aware oracle that selects critical layers via direct task-sensitivity tests, assigning precision according to observed degradation.
- **Empirical results**: across code, math, and trivia tasks on open-weight LLMs, TAQ maintains accuracy within ≤ 1 point of full precision while reducing model size and latency.

The remainder of this paper is organized as follows. §2 reviews post-training quantization, layer-wise activations, and related background. §3 introduces TAQ, its motivation, and the scoring and allocation procedures. §4 reports experimental results. Finally, §5 discusses implications, limitations, and future directions.

2. Background and Related Work

Recent work indicates that different tasks rely on different layers, with some layers carrying stronger task-specific signals (Evcı et al., 2022; Burns et al., 2023). These findings enable weight-space editing via task vectors (Iiharco et al., 2023) and behavioral steering through hidden-activation interventions (Turner et al., 2023b; Zou et al., 2023a). In parallel, advances in PTQ have achieved low-bit inference from small calibration sets via high-fidelity rounding, range equalization, activation-aware precision allocation, representation-space rotations, and cache compression (Frantar et al., 2022; Xiao et al., 2023; Lin et al., 2023a; Shao et al., 2024; Ashkboos et al., 2024; Liu et al., 2024b; Hooper et al., 2024; He et al., 2024). Despite their effectiveness, these methods are largely task-agnostic: they optimize

layer-local error surrogates on generic calibration data rather than end-task metrics, and they do not exploit task-specific activation signals. We adopt a task-conditioned perspective that uses per-layer evidence from hidden representations to guide precision allocation, linking PTQ techniques with semantic analyses of internal representations.

Quantization: from uniform to layer- and activation-aware. LLMs are typically composed of N stacked Transformer blocks (Vaswani et al., 2017). For block i , let $a_i(\cdot)$ denote hidden activations. On modern hardware, inference is often constrained by memory bandwidth and latency rather than raw FLOPs (Dao et al., 2022; Kwon et al., 2023). Quantization addresses these limitations by mapping floating-point tensors to lower-precision representations, thereby reducing memory footprint and improving throughput. A standard (asymmetric) uniform PTQ scheme applies

$$Q(x) = \text{round}\left(\frac{x - z}{s}\right) \cdot s + z,$$

where s is a scale and z a zero-point offset (Nagel et al., 2021; Jacob et al., 2018; Krishnamoorthi, 2018).

Beyond global uniformity, advances proceed along three axes: (i) *weight-only PTQ and rounding*, including GPTQ (local-loss-aware rounding), LLM.INT8 (activation-outlier handling), SmoothQuant (weight-activation trade-off), and OmniQuant/RPTQ (compensation and reordering) (Frantar et al., 2022; Dettmers et al., 2022; Xiao et al., 2023; Shao et al., 2024; Yuan et al., 2023); (ii) *sensitivity-driven bit allocation* under a global budget using curvature or error models (Dong et al., 2019; Yao et al., 2022; 2023; Sharify et al., 2024); and (iii) *activation- and channel-aware calibration* that preserves salient channels/heads and increasingly targets the KV cache for long context (Lin et al., 2023a; Xiao et al., 2023; Shao et al., 2024; Yuan et al., 2023; Liu et al., 2024a). Within the last category, **AWQ** (Activation-aware Weight Quantization) is particularly influential: it calibrates decisions using both weight distributions and activation statistics, explicitly preserving activation outliers critical to LLM accuracy, and thereby achieves effective compression and acceleration with minimal downstream degradation (Lin et al., 2023a).

Per-layer activation analysis and directionality. A complementary line of work analyzes the geometry of hidden activations: linear directions have been shown to encode semantic features and afford inference-time control (Turner et al., 2023a; Zou et al., 2023b), while localized edits can reveal and manipulate factual computation (Meng et al., 2022). Let $\mathcal{B} = \{B_1, \dots, B_M\}$ denote benchmarks (tasks), and for task k let $D_k = \{(q_j, a_j)\}_{j=1}^{n_k}$ be a labeled set. A

task-conditioned direction at layer i can be estimated as

$$d_i^{(k)} = \frac{1}{n_k} \sum_{(q_j, a_j) \in D_k} (a_i(q_j) - a_i(\tilde{q}_j)),$$

where \tilde{q}_j are contrast prompts, and cross-task alignment can be measured by the cosine similarity

$$s_i^{(k, \ell)} = \frac{\langle d_i^{(k)}, d_i^{(\ell)} \rangle}{\|d_i^{(k)}\| \|d_i^{(\ell)}\|}.$$

Per-layer activation (PLA) analyses (Skean et al., 2025) relate layer-local norms, sparsity, and directionality to downstream performance, suggesting that compression and precision budgets should follow where task-salient signal resides (Turner et al., 2023a; Meng et al., 2022; Arditi et al., 2024; Levi et al., 2025a;b).

Layer hidden representations. Understanding how information is organized across layers requires a diagnostic that distinguishes compressed from diverse representations. A convenient approach is to examine the spectrum of the token–token Gram matrix, which reflects how hidden states spread across directions at each depth. Let $X_\ell \in \mathbb{R}^{n \times d}$ denote hidden states at layer ℓ , and define $K_\ell = \frac{1}{n} X_\ell X_\ell^\top$ with eigenvalues $\{\lambda_i\}_{i=1}^n$. Using normalized eigenvalues $\tilde{\lambda}_i = \lambda_i / \sum_{j=1}^n \lambda_j$, the (Shannon) matrix entropy

$$H(K_\ell) = - \sum_{i=1}^n \tilde{\lambda}_i \log \tilde{\lambda}_i$$

quantifies dispersion: larger values indicate more isotropic (diverse) token representations, whereas smaller values indicate concentration (compression). Recent analyses unify information-theoretic, geometric, and invariance-based diagnostics for hidden states and find that intermediate layers often yield stronger, more task-useful features than the final layer, exhibiting a mid-depth “compression valley” that correlates with downstream performance across models and domains (Skean et al., 2025).

Task signals within LLM activation space. Task-conditioned compression concentrates precision on representations that matter for a target task distribution. Given a task-specific calibration set $C_k \subseteq \mathcal{D}$, we compute per-layer relevance scores $r_i^{(k)}$ (e.g., direction norms or projection energies) from hidden activations and then solve a budgeted allocation problem:

$$\min_{\mathbf{b} \in \mathcal{B}} \mathcal{E}_k(\mathbf{b}) \quad \text{s.t.} \quad \text{Cost}(\mathbf{b}) \leq \tau,$$

where $\mathbf{b} = (b_1, \dots, b_N)$ are per-layer bitwidths, \mathcal{E}_k is a task-conditioned error proxy (e.g., task loss on C_k or a sensitivity surrogate), and τ enforces a memory/latency budget via $\text{Cost}(\cdot)$ (e.g., model size or estimated throughput). This formulation prioritizes layers with high $r_i^{(k)}$ by allocating higher precision where task-salient signal is concentrated.

External representation alignment and invariances. Beyond PTQ, work on latent-space geometry shows that aligning representations and exploiting invariances can improve efficiency. Moschella et al. (2022) propose manifold-product and relative-representation methods that enable zero-shot model stitching across tasks; Löhner & Moeller (2024) demonstrate alignment and anchoring techniques using linear maps and invariances; Dominé et al. (2024) examine representation dynamics in linear networks; Zhao et al. (2023) explore parameter symmetries for data-free quantization; and Williams et al. (2021) introduce shape metrics to compare neural representations. Together, these insights underscore the importance of latent-space structure for efficient models and motivate our task-aware quantization.

Connecting PTQ with representation analyses. We address the task-agnostic gap in PTQ by linking methods that optimize quantization objectives and allocate per-layer bit precision (e.g., Lin et al. (2023a)) with advances in mechanistic interpretability and semantic analyses of hidden representations (Skean et al., 2025). Concretely, we instantiate PTQ with task-informed surrogates and per-layer allocation rules derived from representation diagnostics, yielding a high-performance, task-oriented quantization approach.

3. Method

We introduce **TAQ**, a task-aware post-training quantization framework that assigns mixed precision across Transformer layers using task-conditioned activation statistics. This section is organized as follows. §3 motivates a task-aware view and formalizes the budgeted objective. §3.1 details **TAQ**’s two components: (i) layer relevance scoring and (ii) a lightweight calibration procedure that tunes quantizer parameters on a small, task-specific calibration set. Finally, §3.2 presents **TAQO**, an oracle-style variant that selects high-precision layers via task-specific sensitivity.

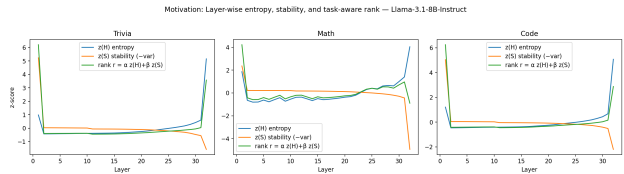


Figure 1. Layers relevance scores per task.

Motivation. Different tasks stress different parts of a Transformer: some layers are indispensable for capturing semantic diversity, while others can be aggressively quantized with little effect. In Figure 1, we show per-layer relevance signals for Llama-3.1-8B-Instruct across TriviaQA (Joshi et al., 2017) (open-domain question answering with

evidence documents), GSM8K (Cobbe et al., 2021a) (grade-school math word problems requiring multi-step reasoning), and MBPP (Austin et al., 2021) (Python code synthesis from natural-language prompts with unit tests), measured via prompt entropy H_ℓ , stability $S_\ell = -\text{Var}(X_\ell)$, and a combined rank $r_\ell = \alpha z(H_\ell) + \beta z(S_\ell)$. The resulting profiles are task-dependent: TriviaQA and MBPP concentrate importance near input/output boundaries (early lexical grounding and late semantic control), whereas GSM8K exhibits a broad mid-to-late plateau where entropy grows and stability drops, reflecting the need to preserve intermediate reasoning structure. Mid-layers in TriviaQA and MBPP are comparatively flat and redundant, tolerating more aggressive quantization. Relevance is therefore neither uniform nor universal, motivating task-aware allocation that assigns higher precision where task-specific signals concentrate.

Objective. Let a pretrained model with N Transformer layers and parameters θ be given, and let \mathcal{D} denote the target data distribution. Post-training quantization seeks a compressed parameterization $\hat{\theta}$ that respects a resource budget while preserving task performance:

$$\min_{\hat{\theta} \in \mathcal{Q}(\theta)} \mathbb{E}_{x \sim \mathcal{D}} [\mathcal{L}(f_\theta(x), f_{\hat{\theta}}(x))] \quad \text{s.t.} \quad \text{Cost}(\hat{\theta}) \leq \tau, \quad (1)$$

where $\mathcal{Q}(\theta)$ is the family of quantized models derived from θ , \mathcal{L} measures discrepancy (e.g., between logits or intermediate activations), and $\text{Cost}(\cdot)$ encodes memory/latency constraints with budget τ .

Let $\mathbf{b} = (b_1, \dots, b_N)$ denote per-layer bitwidths chosen from an admissible set \mathcal{B} (e.g., low/medium/high precision). Given a small calibration set $\mathcal{C} \subset \mathcal{D}$, we formulate task-aware mixed precision as

$$\min_{\mathbf{b} \in \mathcal{B}^N, \phi} \mathcal{E}(\mathbf{b}, \phi; \mathcal{C}) \quad \text{s.t.} \quad \text{Cost}(\mathbf{b}) \leq \tau, \quad (2)$$

where ϕ collects quantizer parameters (e.g., scales and zero-points), and \mathcal{E} is a proxy error that upper-bounds the discrepancy in (1) when quantizing with (\mathbf{b}, ϕ) . The key design choice is to *allocate larger bitwidth to layers whose activations are both informative and stable for the task*.

3.1. Task-Aware Quantization (TAQ)

TAQ proceeds in two stages. First, each layer ℓ receives a relevance score R_ℓ computed from task-conditioned activation statistics; these scores guide the bitwidth allocation \mathbf{b} under the resource budget. Second, with \mathbf{b} fixed, the quantizer parameters ϕ are calibrated on \mathcal{C} to minimize the mismatch between full-precision and quantized behavior.

Scoring: information and stability. For input x , let $X_\ell(x) \in \mathbb{R}^{T \times d_\ell}$ denote activations at layer ℓ . From a

small reservoir $\{v_i\}_{i=1}^{r_\ell} \subset \mathbb{R}^{d_\ell}$ sampled across \mathcal{C} , construct the centered matrix Z_ℓ and the Gram matrix $K_\ell = \frac{1}{r_\ell} Z_\ell Z_\ell^\top$. With eigenvalues $\{\lambda_i\}$ and normalized spectrum $\tilde{\lambda}_i = \lambda_i / \sum_j \lambda_j$, define the *information score*

$$H_\ell = - \sum_i \tilde{\lambda}_i \log \tilde{\lambda}_i, \quad (3)$$

which quantifies representational diversity. In parallel, maintain streaming moments $(S_\ell^{(1)}, S_\ell^{(2)}, n_\ell)$ over token activations and define

$$\text{Var}_\ell = \frac{S_\ell^{(2)}}{n_\ell} - \left(\frac{S_\ell^{(1)}}{n_\ell} \right)^2, \quad S_\ell = -\text{Var}_\ell, \quad (4)$$

so lower variance yields higher *stability*. After z -scoring across layers, the task-conditioned relevance is

$$R_\ell = \alpha \widehat{H}_\ell + \beta \widehat{S}_\ell, \quad \alpha, \beta \geq 0, \quad \alpha + \beta = 1, \quad (5)$$

and layers are ranked by R_ℓ to guide the constrained allocation in (2).¹

Calibration: quantizer tuning. Let \mathcal{W}_ℓ be the set of weight matrices in layer ℓ . For a chosen bitwidth $b_\ell \in \mathcal{B}$, each weight group $W_g \subset \mathcal{W}_\ell$ is mapped to integer codes by a parametric quantizer q_{b_ℓ, ϕ_g} with parameters ϕ_g (e.g., scale and offset). Denote the quantized model by $f_{\hat{\theta}(\mathbf{b}, \phi)}$. With \mathbf{b} fixed, **TAQ** calibrates ϕ via a small optimization on \mathcal{C} :

$$\min_{\phi} \sum_{x \in \mathcal{C}} \mathcal{L}(f_\theta(x), f_{\hat{\theta}(\mathbf{b}, \phi)}(x)), \quad (6)$$

where \mathcal{L} may compare logits and/or intermediate activations. This tunes only ϕ while keeping θ frozen, yielding a task-conditioned quantized model that satisfies the budget τ and preserves downstream performance.

3.2. Task-Aware Quantization with Oracle Layer Selection (TAQO)

While **TAQ** assigns precision by ranking continuous relevance signals (H_ℓ, S_ℓ) , it is also useful to study a discrete, *oracle-style* baseline that leverages direct task-specific sensitivity. We denote this variant **TAQO**. For each task, identify a subset of layers $\mathcal{K}_t \subseteq \{1, \dots, N\}$ that are empirically *critical*, as determined by performance degradation when they alone are quantized to low precision. These layers are preserved at high precision, while the remainder are quantized to the target bitwidth.

Formally, let Δ_ℓ denote the task-level performance drop when layer ℓ is quantized while all other layers remain full precision. For task t , the set of critical layers is

$$\mathcal{K}_t = \{\ell \mid \Delta_\ell \geq \gamma\}, \quad (7)$$

¹In practice, the allocation reduces to a monotone knapsack under a global bit budget.

where γ is a task-dependent sensitivity threshold. The bit allocation rule then becomes

$$b_\ell = \begin{cases} b_{\text{high}}, & \ell \in \mathcal{K}_t, \\ b_{\text{low}}, & \text{otherwise,} \end{cases} \quad b_{\text{high}} > b_{\text{low}}, \text{ Cost}(\mathbf{b}) \leq \tau. \tag{8}$$

By construction, **TAQO** provides an optimistic *upper bound* on task-aware allocation under a given budget. Empirically, \mathcal{K}_t varies substantially across tasks, underscoring that quantization tolerance is not layer-uniform but task-dependent. Although impractical for deployment—since it presumes access to sensitivity curves—**TAQO** serves as a valuable ceiling that motivates lightweight proxies.

4. Experiments

Overview. We empirically study task-aware mixed-precision quantization on LLMs across QA-style workloads. Our central hypothesis is that *task-salient evidence is unevenly distributed across layers*, hence precision should follow where this evidence resides. We compare our methods against representative baselines. **AWQ** (Activation-aware Weight Quantization) calibrates quantization by preserving activation outliers critical to performance, using a small *mixed-task* pool following the original recipe (Lin et al., 2023b; 2024). **AWQ-OT** applies the same procedure but uses a *single task-specific* calibration set identical to that used by our methods. Our proposed **TAQ** allocates precision based on hidden-representation statistics computed on a task-specific calibration set, while **TAQO** uses oracle sensitivity curves in place of surrogate statistics (i.e., **TAQ** with oracle-derived relevance).

Research questions.

- Representation differences.** Do prompt representations *in task context* evolve differently across depth for different tasks, inducing distinct task-specific precision profiles?
- AWQ vs. AWQ-OT.** Does task-specific calibration (AWQ-OT) improve over mixed-pool AWQ despite the same quantization rule?
- AWQ-OT vs. TAQ/TAQO.** Do task-aware scoring (**TAQ**) or oracle sensitivities (**TAQO**) outperform AWQ-OT, indicating that task-aware allocation is the key ingredient?
- Effectiveness.** Under the same budget, do **TAQ** and **TAQO** achieve higher accuracy than activation-aware baselines, and how do they differ in practice?

4.1. Experimental Settings

Models. We evaluate open-weight LLMs representative of current practice: *Llama-3.1-8B Instruct* (Dubey & et al., 2024), *Qwen3-4B Instruct* and *Qwen2.5-7B Instruct* (Team, 2024), *Mistral-7B Instruct* (AI, 2023), and *Phi-4-mini Instruct* (Abdin & et al., 2024).

Baselines. $W \setminus O$ denotes the original model without quantization (full precision). **AWQ** uses mixed-task calibration as in the original works (Lin et al., 2023b; 2024). **AWQ-OT** uses the identical AWQ recipe but with a single task-specific calibration set matching that of **TAQ/TAQO**.

Evaluation. We report *Exact Match (EM)* and token-level *F1* (Rajpurkar et al., 2016).

Datasets and calibration. Our main evaluation task is *TriviaQA*. For task-specific calibration we use 512 examples per setting. For mixed calibration, we form an equal-sized pool drawn from *math*, *trivia*, and *code* prompts (total 2048 examples; balanced across the three).

Implementation and reproducibility. Experiments run on 8x A40 NVIDIA GPUs. Unless stated otherwise, generation uses greedy decoding (`do_sample=False`) with `max_new_tokens=64`, `score_max_texts=256`, `score_max_tokens=512`, and batch size 8. For our methods, defaults are: reservoir size 256; scoring batch size 8; information/variance weights $(\alpha, \beta) = (0.5, 0.5)$; first/last two layers left at $W \setminus O$; mid-layer budgets selected automatically (approximately 15% of non-edge layers at 16-bit and 45% at 8-bit by rank); per-group size 128; cached dequantization enabled.

4.2. Experimental Results

We first compare depth profiles under task-specific calibration pools (Section 3). We observe sharp cross-task differences in the distribution of task-salient signals, arguing against uniform bitwidth allocation and motivating task-aware precision assignment.

Restricting AWQ calibration to the target task (**AWQ-OT**) improves over mixed-pool AWQ on some models (e.g., Qwen2.5 and Mistral-7B), but gains are inconsistent and sometimes negligible. On *Phi-4*, AWQ-OT collapses (0.73 EM / 4.54 F1), indicating that calibration alone cannot ensure stability without task-aware layer selection.

Both **TAQ** and **TAQO** outperform AWQ-OT across models. On *Phi-4*, **TAQ** preserves near- $W \setminus O$ accuracy (42.33 EM / 50.81 F1 vs. 43.16 / 51.24), a margin of +41.6 EM and +46.3 F1 over AWQ-OT. On *Qwen3*, **TAQ** attains 11.82 / 26.12 (within ≤ 1 point of $W \setminus O$), while **TAQO** reaches 18.51 / 34.34, illustrating the benefit of oracle layer protec-

Table 1. TriviaQA results (Exact Match and F1). “W\O” denotes performance *without quantization*. For each model, the best quantized result is **bolded** and the second-best is underlined.

Method	Phi-4		Qwen3		Llama-3.1		Qwen2.5		Mistral	
	EM	F1								
W\O	43.16	51.24	11.23	26.33	57.86	66.00	11.43	21.90	18.90	35.18
TAQO (Ours)	0.73	4.57	18.51	34.34	57.91	<u>65.14</u>	12.65	25.49	<u>18.51</u>	<u>34.34</u>
TAQ (Ours)	42.33	50.81	<u>11.82</u>	<u>26.12</u>	<u>57.03</u>	65.35	<u>12.06</u>	22.47	18.75	34.74
AWQ	<u>2.25</u>	<u>7.07</u>	9.23	23.94	53.37	62.23	11.91	24.06	17.48	33.75
AWQ-OT	0.73	4.54	9.81	24.33	55.66	62.92	10.59	<u>24.21</u>	17.58	26.33

tion. On *Llama-3.1*, **TAQ** nearly matches W\O (57.03 / 65.35 vs. 57.86 / 66.00) and surpasses AWQ and AWQ-OT; **TAQO** slightly improves F1 (57.91 / 65.14). On *Qwen2.5*, **TAQ** yields 12.06 / 22.47, and **TAQO** improves to 12.65 / 25.49. Finally, on *Mistral*, **TAQ** posts 18.75 / 34.74, closely tracking W\O (18.90 / 35.18) and surpassing AWQ-OT (17.58 / 26.33).

Across models, **TAQ** offers a stronger Pareto frontier than baselines: accuracy remains within ≤ 1 EM/F1 point of W\O while reducing memory and latency. **TAQO** validates the layer-selection principle by reaching or exceeding W\O on some settings (e.g., Qwen3), confirming that protecting critical layers is the right axis of optimization. Together, the results show that task-aware precision—guided by proxy signals or oracle sensitivities—yields stable and efficient quantization.

Takeaways. (1) Task-specific representation profiles differ across domains, requiring task-aware allocation. (2) AWQ-OT improves on some models but remains unstable on others (e.g., *Phi-4*), indicating that task-specific calibration alone is insufficient without task-aware layer selection. (3) **TAQ** consistently recovers near-W\O accuracy with large efficiency gains; **TAQO** can further improve accuracy, supporting the underlying layer-selection principle.

5. Conclusions

We explored task-aware mixed-precision quantization for LLMs, asking whether precision should follow where task evidence resides. We found that layerwise profiles vary systematically across domains: TriviaQA tends to peak late; MBPP concentrates mid-to-late; and GSM8K exhibits a broader distribution—clarifying why task-agnostic PTQ often misallocates precision. **TAQ** addresses this by coupling entropy- and stability-based signals with a budgeted allocator, consistently preserving near-W\O accuracy within ≤ 1 point (e.g., Llama-3.1: 57.03/65.35 vs. 57.86/66.00; Phi-4: 42.33/50.81 vs. 43.16/51.24), while outperforming activation-aware baselines such as AWQ. Compared to task-

calibrated AWQ (AWQ-OT), **TAQ** avoids catastrophic collapse (Phi-4: 0.73/4.54 under AWQ-OT) and delivers stable gains.

In addition, **TAQO** establishes an upper bound by perfectly retaining critical layers and, in some cases, surpasses W\O accuracy (Qwen3: 18.51/34.34 vs. 11.23/26.33), confirming that task-specific sensitivity is decisive. While impractical for deployment, **TAQO** validates the premise for lightweight proxies, showing that quantization can serve not only as compression but also as a lens on how tasks are encoded across depth.

Beyond efficiency, the interpretability angle is notable: task-conditioned profiles surface representational “pressure points” aligned with task-salient computation, turning quantization into a tool for both compression and probing hidden structure. Limitations include dependence on small calibration sets and sensitivity to deployment hardware. Promising directions include dynamic, input-conditioned bit schedules and multi-task allocation. Overall, our method demonstrates that lightweight, task-conditioned signals can preserve accuracy where it matters most.

References

Abdin, M. and et al. Phi-4 technical report. *arXiv preprint arXiv:2412.08905*, 2024. URL <https://arxiv.org/abs/2412.08905>.

AI, M. Mistral 7b. <https://mistral.ai/news/announcing-mistral-7b/>, 2023.

Arditi, A., Roberts, O., Stewart, A., Turner, A., and Thiergart, J. Refusal in language models is mediated by a single direction. In *arXiv preprint arXiv:2406.11717*, 2024.

Ashkboos, S., Frantar, E., Hoefler, T., and Alistarh, D. Quarot: Quantization with rotation for large language models. *arXiv preprint arXiv:2404.00456*, 2024. URL <https://arxiv.org/abs/2404.00456>.

- Austin, J., Odena, A., Nye, M., Bosma, M., Michalewski, H., Dohan, D., Jiang, E., Cai, C., Terry, M., Le, Q., et al. Program synthesis with large language models. *arXiv preprint arXiv:2108.07732*, 2021.
- Banner, R., Nahshan, Y., and Soudry, D. Post training 4-bit quantization of convolutional networks for rapid-deployment. *Advances in neural information processing systems*, 32, 2019.
- Bowen, J., Freedman, S., Zhang, Z., and Belinkov, Y. Selective task arithmetic: Per-vector selection for robust model editing and merging. In *Proceedings of the 41st International Conference on Machine Learning (ICML Workshop/Proceedings Track)*, 2024. URL <https://arxiv.org/abs/2404.03592>. arXiv:2404.03592.
- Burns, C., Ye, H., Klein, D., and Steinhardt, J. Discovering latent knowledge in language models without supervision. In *International Conference on Learning Representations*, 2023. URL <https://openreview.net/forum?id=0c-S0RyWhq>.
- Chen, M. et al. Evaluating large language models trained on code. *arXiv preprint arXiv:2107.03374*, 2021.
- Cobbe, K., Kosaraju, V., Bavarian, M., Chen, M., Jun, H., Kaiser, L., Plappert, M., Tworek, J., Hilton, J., Nakano, R., et al. Training verifiers to solve math word problems. *arXiv preprint arXiv:2110.14168*, 2021a.
- Cobbe, K. et al. Training verifiers to solve math word problems. *arXiv preprint arXiv:2110.14168*, 2021b.
- Dao, T., Fu, D. Y., Ermon, S., Rudra, A., and Ré, C. FlashAttention: Fast and memory-efficient exact attention with IO-awareness. In *Advances in Neural Information Processing Systems (NeurIPS)*, 2022. URL <https://openreview.net/forum?id=JENyE4ZG5b>.
- Dettmers, T., Lewis, M., Belkada, Y., and Zettlemoyer, L. Llm.int8(): 8-bit matrix multiplication for transformers at scale. In *Advances in Neural Information Processing Systems (NeurIPS)*, 2022. URL <https://arxiv.org/abs/2208.07339>.
- Dominé, C. C., Anguita, N., Proca, A. M., Braun, L., Kunin, D., Mediano, P. A., and Saxe, A. M. From lazy to rich: Exact learning dynamics in deep linear networks. *arXiv preprint arXiv:2409.14623*, 2024.
- Dong, Z., Yao, Z., Gholami, A., Mahoney, M. W., and Keutzer, K. Hawq: Hessian aware quantization of neural networks with mixed-precision. In *Proceedings of the IEEE/CVF International Conference on Computer Vision (ICCV)*, pp. 293–302, 2019.
- Dubey, A. and et al. The llama 3 herd of models. *arXiv preprint arXiv:2407.21783*, 2024. URL <https://arxiv.org/abs/2407.21783>.
- Evci, U., Dumoulin, V., Laroche, H., and Mozer, M. C. Head2toe: Utilizing intermediate representations for better transfer learning. In *Proceedings of the 39th International Conference on Machine Learning*, volume 162 of *Proceedings of Machine Learning Research*. PMLR, 2022. URL <https://proceedings.mlr.press/v162/evci22a.html>.
- Frantar, E., Ashkboos, S., Hoefler, T., and Alistarh, D. Gptq: Accurate post-training quantization for generative pretrained transformers. In *Proceedings of the International Conference on Learning Representations (ICLR)*, 2022.
- Gholami, A., Kim, S., Dong, Z., Yao, Z., Mahoney, M. W., and Keutzer, K. A survey of quantization methods for efficient neural network inference. *arXiv preprint arXiv:2103.13630*, 2021. URL <https://arxiv.org/abs/2103.13630>.
- He, . et al. Zipcache: Byte-level kv cache compression for transformer inference. In *Advances in Neural Information Processing Systems (NeurIPS)*, 2024. URL https://proceedings.neurips.cc/paper_files/paper/2024/file/7e57131fdeb815764434b65162c88895-Paper-Conference.pdf.
- Hendrycks, D. and et al. MATH: Measuring mathematical problem solving with the MATH dataset. *arXiv preprint arXiv:2103.03874*, 2021. URL <https://arxiv.org/abs/2103.03874>.
- Hinton, G., Vinyals, O., and Dean, J. Distilling the knowledge in a neural network. *arXiv preprint arXiv:1503.02531*, 2015. URL <https://arxiv.org/abs/1503.02531>.
- Hoffmann, J., Borgeaud, S., Mensch, A., Buchatskaya, E., Cai, T., Rutherford, E., Casas, D., Welbl, J., Clark, A., Hennigan, T., et al. Training compute-optimal large language models. *arXiv preprint arXiv:2203.15556*, 2022. URL <https://arxiv.org/abs/2203.15556>.
- Hooper, R. et al. Kvquant: Towards general and efficient kv-cache quantization for large language models. In *Advances in Neural Information Processing Systems (NeurIPS)*, 2024. URL <https://nips.cc/virtual/2024/poster/97760>.
- Hu, E. J., Shen, Y., Wallis, P., Allen-Zhu, Z., Li, Y., Wang, S., Wang, L., and Chen, W. Lora: Low-rank adaptation of large language models. *arXiv preprint arXiv:2106.09685*, 2021. URL <https://arxiv.org/abs/2106.09685>.

- Iharcó, G., Ribeiro, M. T., Wortsman, M., Gururangan, S., Schmidt, L., Hajishirzi, H., and Farhadi, A. Editing models with task arithmetic. In *International Conference on Learning Representations*, 2023. URL <https://arxiv.org/abs/2212.04089>.
- Jacob, B., Kligys, S., Chen, B., Zhu, M., Tang, M., Howard, A., Adam, H., and Kalenichenko, D. Quantization and training of neural networks for efficient integer-arithmetic-only inference. In *Proceedings of the IEEE/CVF Conference on Computer Vision and Pattern Recognition (CVPR)*, pp. 2704–2713, 2018. URL https://openaccess.thecvf.com/content_cvpr_2018/html/Jacob_Quantization_and_Training_CVPR_2018_paper.html.
- Joshi, M., Choi, E., Weld, D. S., and Zettlemoyer, L. Triviaqa: A large scale distantly supervised challenge dataset for reading comprehension. In *Proceedings of the 55th Annual Meeting of the Association for Computational Linguistics (Volume 1: Long Papers)*, pp. 1601–1611, 2017.
- Kaplan, J., McCandlish, S., Henighan, T., Brown, T. B., Chess, B., Child, R., Gray, S., Radford, A., Wu, J., and Amodei, D. Scaling laws for neural language models. *arXiv preprint arXiv:2001.08361*, 2020. URL <https://arxiv.org/abs/2001.08361>.
- Krishnamoorthi, R. Quantizing deep convolutional networks for efficient inference: A whitepaper. *arXiv preprint arXiv:1806.08342*, 2018. URL <https://arxiv.org/abs/1806.08342>.
- Kwon, W., Li, Z., Zhuang, S., Sheng, Y., Zheng, L., Yu, C. H., Gonzalez, J. E., Zhang, H., and Stoica, I. Efficient memory management for large language model serving with pagedattention. *arXiv preprint arXiv:2309.06180*, 2023. URL <https://arxiv.org/abs/2309.06180>.
- Lähler, Z. and Moeller, M. On the direct alignment of latent spaces. In *Proceedings of UniReps: the First Workshop on Unifying Representations in Neural Models*, pp. 158–169. PMLR, 2024.
- Levi, A., Himelstein, R., Nemcovsky, Y., Mendelson, A., and Baskin, C. Enhancing jailbreak attacks via compliance-refusal-based initialization. *arXiv e-prints*, pp. arXiv–2502, 2025a.
- Levi, A., Himelstein, R., Nemcovsky, Y., Mendelson, A., and Baskin, C. Jailbreak attack initializations as extractors of compliance directions. *arXiv preprint arXiv:2502.09755*, 2025b.
- Li, S., Yao, L., Zhang, L., and Li, Y. Safety layers in aligned large language models: The key to llm security. *arXiv preprint arXiv:2408.17003*, 2024. URL <https://arxiv.org/abs/2408.17003>. ICLR 2025 (OpenReview).
- Lin, J., Tang, J., Tang, H., Yang, S., Dang, X., and Han, S. Awq: Activation-aware weight quantization for llm compression and acceleration. In *Proceedings of the Conference on Neural Information Processing Systems (NeurIPS)*, 2023a.
- Lin, J., Tang, J., Tang, H., Yang, S., et al. AWQ: Activation-aware weight quantization for llm compression and acceleration. *arXiv preprint arXiv:2306.00978*, 2023b. URL <https://arxiv.org/abs/2306.00978>.
- Lin, J., Tang, H., Li, Z., Zhang, H., et al. AWQ: Activation-aware weight quantization for on-device llm compression and acceleration. In *MLSys*, 2024. URL https://proceedings.mlsys.org/paper_files/paper/2024/file/42a452cbafa9dd64e9ba4aa95cc1ef21-Paper-Conference.pdf.
- Liu, Z., Yuan, J., Jin, H., Zhong, S., Xu, Z., Braverman, V., Chen, B., and Hu, X. KIVI: A tuning-free asymmetric 2bit quantization for KV cache. In *Proceedings of the 41st International Conference on Machine Learning (ICML)*, volume 235 of *Proceedings of Machine Learning Research*, 2024a. URL <https://proceedings.mlr.press/v235/liu24bz.html>.
- Liu, Z., Zhao, C., Fedorov, I., Soran, B., Choudhary, D., Krishnamoorthi, R., Chandra, V., Tian, Y., and Blankevoort, T. Spinqant: Llm quantization with learned rotations. *arXiv preprint arXiv:2405.16406*, 2024b. doi: 10.48550/arXiv.2405.16406. URL <https://arxiv.org/abs/2405.16406>. ICLR 2025.
- Meng, K., Bau, D., Andonian, A., and Belinkov, Y. Locating and editing factual associations in GPT. In *Advances in Neural Information Processing Systems (NeurIPS)*, 2022. URL https://proceedings.neurips.cc/paper_files/paper/2022/file/6f1d43d5a82a37e89b0665b33bf3a182-Paper-Conference.pdf.
- Moschella, L., Maiorca, V., Fumero, M., Norelli, A., Locatello, F., and Rodolà, E. Relative representations enable zero-shot latent space communication. *arXiv preprint arXiv:2209.15430*, 2022.
- Nagel, M., Amjad, R. A., Van Baalen, M., Louizos, C., and Blankevoort, T. Up or down? adaptive rounding for post-training quantization. In *International conference on machine learning*, pp. 7197–7206. PMLR, 2020.

- Nagel, M., Fournarakis, M., Amjad, R. A., and Bondarenko, Y. A white paper on neural network quantization. In *arXiv preprint arXiv:2106.08295*, 2021.
- Ni, R., Sun, S., Xiao, Y.-X., Collins, K., Liu, Z., and Koyejo, S. Quantifying knowledge distillation for large language models and beyond. *arXiv preprint arXiv:2505.13030*, 2025. URL <https://arxiv.org/abs/2505.13030>.
- Ouyang, L., Wu, J., Jiang, X., Almeida, D., Wainwright, C., Mishkin, P., Zhang, C., Agarwal, S., Slama, K., Ray, A., Schulman, J., Hilton, J., Kelton, L., Miller, L., Simens, M., Askell, A., Welinder, P., Christiano, P., Leike, J., and Lowe, R. Training language models to follow instructions with human feedback. In *Advances in Neural Information Processing Systems (NeurIPS)*, 2022. URL <https://arxiv.org/abs/2203.02155>.
- Rajpurkar, P., Jia, R., and Liang, P. SQuAD: 100,000+ questions for machine comprehension of text. In *EMNLP*, 2016. URL <https://arxiv.org/abs/1606.05250>.
- Roziere, B. et al. Code llama: Open foundation models for code. *arXiv preprint arXiv:2308.12950*, 2023.
- Sanh, V., Debut, L., Chaumond, J., and Wolf, T. Distilbert, a distilled version of bert: Smaller, faster, cheaper (and lighter). In *arXiv preprint arXiv:1910.01108*, 2019.
- Shao, W., Chen, M., Zhang, Z., Xu, P., Zhao, L., Li, Z., Zhang, K., Gao, P., Qiao, Y., and Luo, P. OmniQuant: Omnidirectionally calibrated quantization for large language models. In *International Conference on Learning Representations (ICLR)*, 2024. URL <https://arxiv.org/abs/2308.13137>. ICLR 2024 Camera Ready; original preprint arXiv:2308.13137 (2023).
- Sharify, S., Saxena, U., Xu, Z., Yazar, W., Soloveychik, I., and Wang, X. Post training quantization of large language models with microscaling formats. In *Proceedings of The 4th NeurIPS Efficient Natural Language and Speech Processing Workshop (ENLSP-V)*, volume 262 of *Proceedings of Machine Learning Research*, pp. 241–258. PMLR, 2024. URL <https://proceedings.mlr.press/v262/sharify24a.html>.
- Skean, O., Arefin, M. R., Zhao, D., Patel, N., Naghiyev, J., LeCun, Y., and Shwartz-Ziv, R. Layer by layer: Uncovering hidden representations in language models, 2025. URL <https://arxiv.org/abs/2502.02013>.
- Song, R., He, S., Jiang, S., Xian, Y., Gao, S., Liu, K., and Yu, Z. Does large language model contain task-specific neurons? In *Proceedings of the 2024 Conference on Empirical Methods in Natural Language Processing*, 2024. URL <https://aclanthology.org/2024.emnlp-main.403/>.
- Team, Q. Qwen2.5 technical report. <https://qwenlm.github.io/blog/qwen2.5/>, 2024.
- Tsatsaronis, G. et al. An overview of the bioasq large-scale biomedical semantic indexing and question answering competition. *BMC Bioinformatics*, 16(1):138, 2015.
- Turner, A., Thiergart, J., Rando, J., Templeton, A., and Hendrycks, D. Steering language models with activation engineering. In *arXiv preprint arXiv:2308.10248*, 2023a.
- Turner, A. M., Thiergart, L., Leech, G., Udell, D., Vazquez, J. J., Mini, U., and MacDiarmid, M. Steering language models with activation engineering. *arXiv preprint arXiv:2308.10248*, 2023b. doi: 10.48550/arXiv.2308.10248. URL <https://arxiv.org/abs/2308.10248>.
- Turner, A. M., Thiergart, L., Leech, G., Udell, D., Vazquez, J. J., Mini, U., and MacDiarmid, M. Activation addition: Steering language models without optimization. *arXiv preprint arXiv:2308.10248*, 2024. URL <https://arxiv.org/abs/2308.10248>.
- Vaswani, A., Shazeer, N., Parmar, N., Uszoreit, J., Jones, L., Gomez, A. N., Kaiser, L. u., and Polosukhin, I. Attention is all you need. In *Proceedings of the 31st Conference on Neural Information Processing Systems (NeurIPS)*, pp. 5998–6008, 2017.
- Wang, P., Chen, Q., He, X., and Cheng, J. Towards accurate post-training network quantization via bit-split and stitching. In *International Conference on Machine Learning*, pp. 9847–9856. PMLR, 2020.
- Williams, A. H., Kunz, E., Kornblith, S., and Linderman, S. Generalized shape metrics on neural representations. *Advances in neural information processing systems*, 34: 4738–4750, 2021.
- Xiao, G., Lin, J., Seznec, M., Wu, H., Demouth, J., and Han, S. Smoothquant: Accurate and efficient post-training quantization for large language models. In *arXiv preprint arXiv:2211.10438*, 2023.
- Yao, Z., Aminabadi, R. Y., Zhang, M., Li, X., Zhang, Z., and Wang, Y. Zeroquant: Efficient and affordable post-training quantization for large-scale transformers. In *Proceedings of the 36th Conference on Neural Information Processing Systems (NeurIPS)*, pp. 31468–31482, 2022.
- Yao, Z., Li, C., Wu, X., Youn, S., and He, Y. A comprehensive study on post-training quantization for large language models. *arXiv preprint arXiv:2303.08302*, 2023. URL <https://arxiv.org/abs/2303.08302>.

- Yuan, Z., Niu, L., Liu, J., Liu, W., Wang, X., Shang, Y., Sun, G., Wu, Q., Wu, J., and Wu, B. Rptq: Reorder-based post-training quantization for large language models. *arXiv preprint arXiv:2304.01089*, 2023. URL <https://arxiv.org/abs/2304.01089>.
- Zeng, H., Liu, S., Zhang, X., Zhu, C., Chen, X., Rivera, C., van Schijndel, M., Saffari, A., Poliak, A., Tsvetkov, Y., and Sedoc, J. Efficient model editing with task vector bases. *arXiv preprint arXiv:2501.09248*, 2025. URL <https://arxiv.org/abs/2501.09248>.
- Zhang, Y., Dong, Y., and Kawaguchi, K. Investigating layer importance in large language models. *arXiv preprint arXiv:2409.14381*, 2024. URL <https://arxiv.org/abs/2409.14381>.
- Zhao, B., Gower, R. M., Walters, R., and Yu, R. Improving convergence and generalization using parameter symmetries. *arXiv preprint arXiv:2305.13404*, 2023.
- Zhou, L., Gao, R., Song, G., Zhou, L., Zha, H., Li, H., and et al. Knowledge distillation of large language models: A survey. *arXiv preprint arXiv:2405.12396*, 2024. URL <https://arxiv.org/abs/2405.12396>.
- Zhu, X., Li, J., Liu, Y., Ma, C., and Wang, W. A survey on model compression for large language models. *arXiv preprint arXiv:2308.07633*, 2023. URL <https://arxiv.org/abs/2308.07633>.
- Zou, A., Phan, L., Chen, S., Campbell, J., Guo, P., Ren, B., Pan, A., Yin, X., Mazeika, M., Dombrowski, A.-K., et al. Representation engineering: A top-down approach to ai transparency. In *arXiv preprint arXiv:2310.01405*, 2023a.
- Zou, A., Wang, Z., Carlini, N., Nasr, M., Kolter, J. Z., Fredrikson, M., et al. Representation engineering: A top-down approach to AI transparency. *arXiv preprint arXiv:2310.01405*, 2023b. URL <https://arxiv.org/abs/2310.01405>.